Available online at www.sciencedirect.com
ScienceDirect
Journal of Power Sources 159 (2006) 656–666
JOURNAL OF POWER SOURCES
www.elsevier.com/locate/jpowsour

General fuel cell hybrid synergies and hybrid system testing status

Wolfgang Winkler [a], Pedro Nehter [a], Mark C. Williams [b,*], David Tucker [b], Randy Gemmen [b]

[a] Hamburg University of Applied Sciences, Hamburg, Germany
[b] U.S. Department of Energy, National Energy Technology Laboratory, Morgantown, WV, USA

Received 24 August 2005; accepted 28 September 2005
Available online 24 January 2006

Abstract

FCT hybrid power systems offer the highest efficiency and the cleanest emissions of all fossil fuelled power. The engineering for the highest possible efficiency at lowest cost and weight depends on general system architecture issues and the performance of the components. Presented in this paper are system studies which provide direction for the most efficient path toward achieving the most beneficial result for this technology. Ultimately, fuel cell-turbine (FCT) hybrid systems applicable to integrated gasification combined cycle power systems will form the basis for reaching the goals for advanced coal-based power generation. The FCT hybrid power island will also be important for the FutureGen plant and will provide new options for carbon dioxide capture and sequestration as well as power and hydrogen generation. The system studies presented in this paper provide insight to current technology 'benchmarks' versus expected benefits from hybrid applications. Discussion is also presented on the effects of different balance of plant arrangements and approaches.

Finally, we discuss the status of US DOE is sponsored projects that are looking to help understand the unique requirements for these systems. One of these projects, Hyper, will provide information on FCT dynamics and will help identify technical needs and opportunities for cycle advancement. The methods studied show promise for effective control of a hybrid system without the direct intervention of isolation valves or check valves in the main pressure loop of the system, which introduce substantial pressure losses, allowing for realization of the full potential efficiency of the hybrid system.

Keywords: Fuel cell; Fuel cell-turbine; Hybrid power systems

1. Introduction

Fuel cell (FC) hybrid systems are energy converters that can potentially reach the highest possible efficiency known. This makes them attractive for a number of applications—ground-based stationary applications, and within aircrafts and ships. The attractiveness of the system depends on cost in general and weight in particular for aircraft applications. Cost and weight are functions of the installed surfaces within the system. The engineering for the highest possible efficiency at lowest cost and weight depends on general system architecture issues and the performance of subcomponents. For many hybrid systems, it is important to keep the excess air low and the system efficiency high to achieve these targets. Integrated reforming and system pressurization can be further steps to increase efficiency. The gas turbine is the most important heat engine used in hybrid fuel cell systems. The specific operational conditions of fuel cell systems lead to specific designs. Actual hybrid testing and development is expected to increase. To support this development, NETL has built a test facility to improve our understanding of both dynamic and static performances of these advanced systems.

2. General thermodynamic background

Fuel cell hybrid systems are any combination of a fuel cell and a heat engine, where the heat engine uses the waste heat of the fuel cell for further power generation. If we assume that the fuel cell is operating reversibly and the heat engine is a Carnot cycle (CC), we get a simplified but nearly reversible cycle that can be used as a reference cycle for such architectures [1,2].

Fig. 1 shows the architecture. The incoming air and fuel are heated by the waste gas of the fuel cell almost to cell temperature. The waste heat of the fuel cell is removed by the Carnot engine. In reality, this simplified reference cycle is generally not

* Corresponding author. Tel.: +1 304 285 474; fax: +1 304 285 4216.
E-mail address: mark.williams@netl.doe.gov (M.C. Williams).

0378-7753/$ – see front matter © 2006 Published by Elsevier B.V.
doi:10.1016/j.jpowsour.2005.09.070

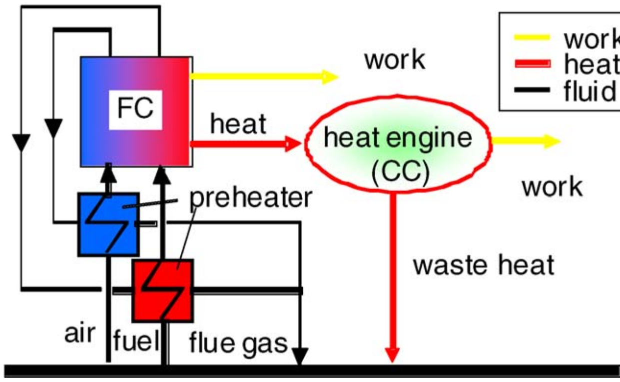

Fig. 1. Simplified fuel cell hybrid reference cycle.

reversible because there are internal losses within the fuel cell, waste heat of the fuel cell is generally needed to heat up the reactants completely and the operation of the heat engine is far less than 100% ideal.

Even so, the knowledge of the behavior of reversible system architecture is the basis of real systems engineering. The use of exergetic efficiencies, the ratio of real work and reversible work, allows the use of reversible architectures to analyze the behavior of real systems independent of the components' detailed design. The Carnot cycle represents any heat engine and the fuel cell, any real fuel cell.

A further simplification of the reference cycle of Fig. 1 leads to a structure as given in Fig. 2 showing the minimum requirements for fuel cell hybrid modeling. The fuel cell is described as a power generating burner supplied with a fuel enthalpy flow $\dot{m}_F \cdot \mathrm{LHV}$ and delivering power P_{elFC} and a certain amount of heat $\dot{Q}_{\mathrm{FC}}$ to the heat engine (HE). The heat engine is delivering the electric power P_{elHE} and waste heat $\dot{Q}_{\mathrm{loss}}$.

It is obvious that the total efficiency of this system only depends on the efficiency of the fuel cell and the efficiency of the heat engine, and there will be a certain 'weighting' of these two efficiencies based on the amount of fuel cell waste heat used by the heat engine. This can be proven easily by a simple energy

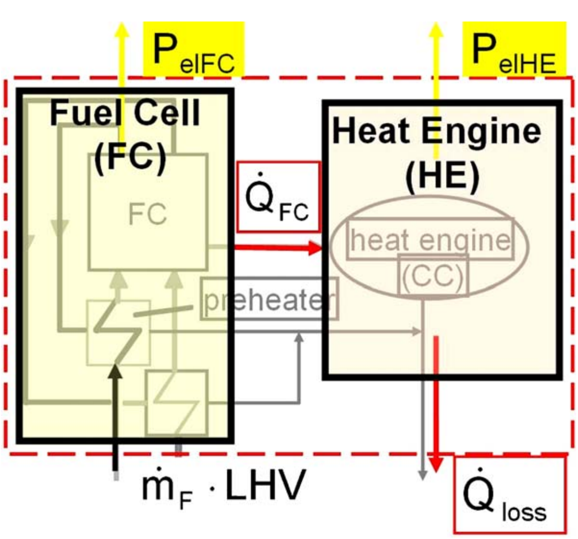

Fig. 2. Simplified FC hybrid calculation.

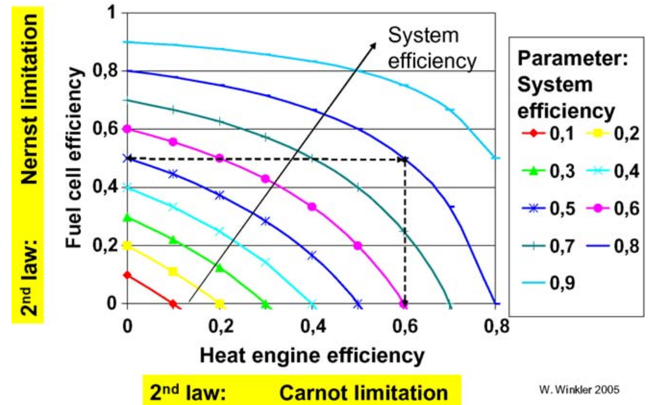

Fig. 3. Generalized FC hybrid efficiency chart.

balance. This approach allows the design of a generalized fuel cell hybrid efficiency chart as shown in Fig. 3.

The *x*-axis of the chart represents the efficiency of the heat engine and the *y*-axis the efficiency of the fuel cell. The resulting system efficiency can be determined as the parameter of the system efficiency curves. The example in the chart shows that we need a heat engine with an efficiency of 60% if we want to reach a system efficiency of 80% with a fuel cell with an efficiency of 50%. This approach only considers the first law. Therefore, the thermodynamic limitation of the second law is expressed at the relevant axis. The fuel cell efficiency is restricted by the Nernst voltage and the efficiency of the heat engine is restricted by the Carnot efficiency. This makes clear that the results of the chart have to be proven by an additional second law consideration.

3. Benchmarks and synergies

In general, the implementation of fuel cells in the energy supply system depends on the expected economic performance of any planned fuel cell project. The resultant fuel cell financing will depend on the particular design selected by the individual fuel cell user. Any utility will be interested in an expected reduction of the actual generation cost by the new planned fuel cell system because the fuel supply is a long term contracted issue. The benchmark is thus the generation cost of actual existing technologies. The expected lower generation cost of the fuel cell system has to finance the project. Any user of the electricity is interested to reduce their electricity cost. The benchmark is then defined by the existing energy market as the price difference between the electricity cost and the gas cost to be contracted. The savings of the energy purchase by reducing the difference between the cost of a local fuel cell generation and the gas price compared to the market will have to finance the fuel cell project [3,4].

Fig. 4 shows an example of such an approach with a ceteris paribus analysis. The benchmark technology CCGT is assumed with an electric efficiency of 55%, a specific investment of US$ 400 kW^{-1} and a depreciation time of 10 years while the SOFC-GT has an electric efficiency of 70% and the same depreciation time. As shown in the figure, the allowable specific investment (capital cost) of the SOFC-GT system depends on the gas price

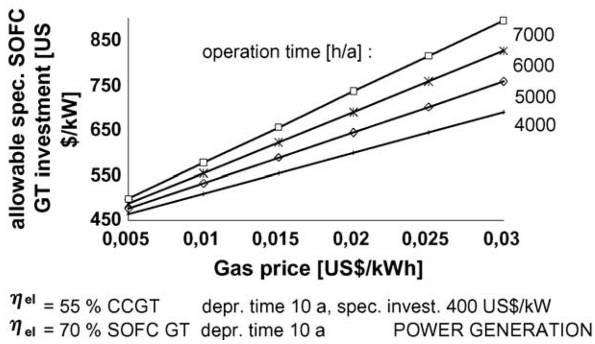

Fig. 4. Allowable specific cost for power generation with a CCGT as a benchmark depending on the gas price. $\eta_{el} = 55\%$ CCGT, depreciation time = 10 years, specific investment = US$ 400 kW^{-1}; $\eta_{el} = 70\%$ SOFC-GT, depreciation time = 10 years power generation.

and the operation time (assumed at full load) which is shown as the parameter in Fig. 4 [3,4].

We see that a high allowable specific investment of the SOFC-GT system of up to nearly 100% is acceptable at a high gas price and a high operation time. But the allowable investment increase is very limited if we assume a low gas price and a low system utilization (i.e., low operation time). The depreciation time of 10 years is used here because this figure is a common one in joint ventures between industries and utilities.

However, costs are still the driving force, and the benchmark in fuel cell development for aircraft is the power density. But if we look on the consequences for engineering we see that the target definition of cost and weight is very similar. Fig. 5 gives an overview.

The system weight depends on the weight of the fuel cell (which depends on the amount of cell area, and the respective wall thickness and density of the material), and the weight of the turbo machinery. The engineering target can be thus defined, which is to find a design solution minimizing the system's area.

The relevant areas can be defined by: (1) the area of the heat exchangers (HEX), (2) the cell area for the transport processes (heat, ions) and (3) the surface of the surroundings (vessel, insulation) of these components. The pipe work including its insulation depends on the flow velocity and the arrangement of the connected components. The process influences are similar to the design of the HEX. Fig. 6 gives an overview.

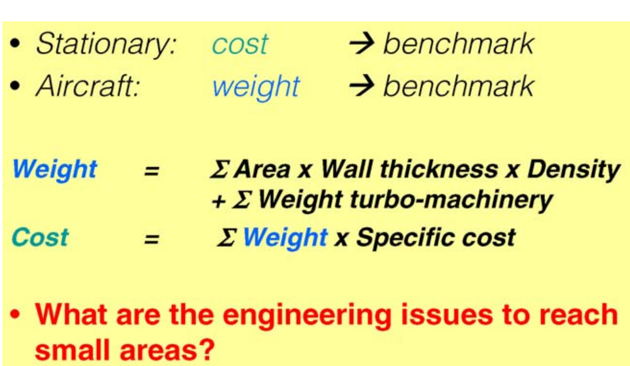

Fig. 5. Fuel cell hybrid benchmark synergies.

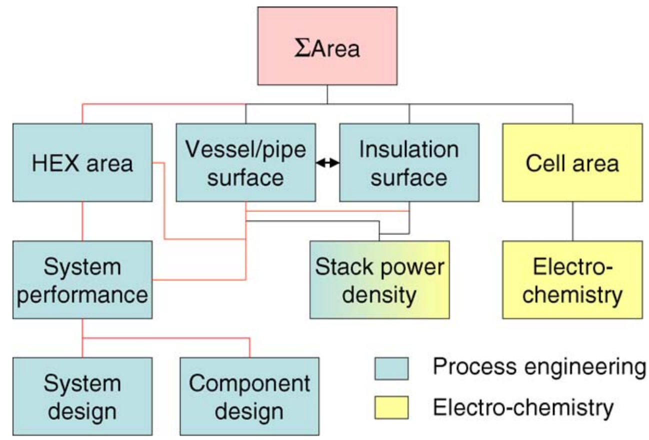

Fig. 6. Influence on the cost and weight relevant areas and surfaces.

The system performance influences the design of the HEX area and the surface of the pipe work by the relevant mass flows, the exchanged heat and the temperature levels. The HEX design and the HEX area influence the relevant vessel surface. The stack power density is the other main issue influencing the vessel surface. The vessel/pipe surfaces and the insulation surfaces are closely connected because the insulation will be between the gases and the wall material in the hot area and outside the wall material in the relative cold parts of the system.

The stack power density depends on design parameters and on electrochemical performance data as well. The cell area itself is assumed to be only dependent of electrochemical performance.

The results of Fig. 6 show that an important part of the cost relevant areas and surfaces depends on the system performance, or in other words of the balance of plant (BoP) behavior. Only the cell area is independent from this approach. The HEX design is the core influence on these areas and surfaces of the HEX itself and the related vessels and insulations. The overall BoP design consists of a system design or architecture defining the BoP structure and the components' design. The system architecture can be described by a certain reference cycle considering the main performance data. This has the benefit that the results of such an examination is independent of a certain technology of the components and thus a general description of hybrid system behavior. The detailed influence of components has to be considered by more complicated models as, e.g., based on Matlab SIMULINK. Fig. 7 shows the influence of the reference cycle and its performance on the HEX area.

The necessary heat recovery determines a certain HEX area necessary for the heat exchange needed. The chosen excess air is obviously another influence on the HEX area. The used HEX efficiency influences the HEX area as well because it determines the amount of heat recovery. But a low HEX efficiency reduces the efficiency of the system, and this increases the fuel needed and thus the mass flows and the HEX surface finally. But the internal reforming is an other method of heat recovery that allows an increase in system efficiency as proven later.

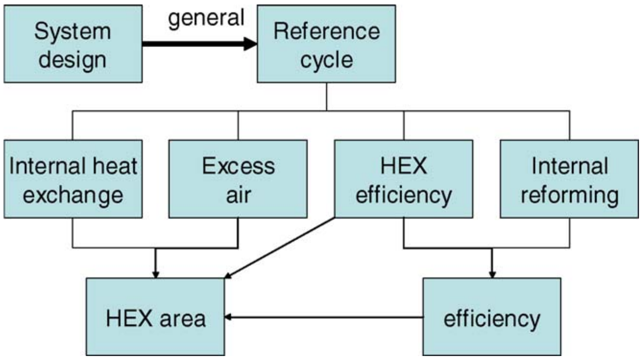

Fig. 7. Influences of the reference cycle on the design of the HEX area.

4. Process engineering (BoP) issues

The system efficiency is principally governed by structural influences of the system architecture and the design of components influences the utilization of the potential of the architecture. The use of hydrocarbons as a fuel and the necessary fuel processing changes the principle system design as shown in Fig. 1. The influence of the component design on the area as a benchmark is the next necessary step to identify the appropriate design.

4.1. General system influence

The following investigations have been done for methane as the main component of natural gas to keep the calculations simple. The thermodynamic principles for other hydrocarbons (e.g., coal syngas which may also contain low but significant amounts of methane) are quite similar; therefore this example can be used here again. A very common fuel processing method for hydrocarbons is the endothermic steam reforming process. The evaporation of the feed water is another heat consumer within the system. The use of the waste heat of the cell is generally a good option for hybrid systems. The combination with a heat engine is a general indication here that the fuel cell waste heat has a sufficiently high temperature. A general model of a methane fired combined SOFC cycle based on the reference cycle of Fig. 1 is shown in Fig. 8 to describe the thermodynamic influences on the system's behavior as simply as possible [4–6]. It can be seen as a general model to study the behavior of a fuel cell hybrid system.

The SOFC can be modeled as one unit of two parallel operating SOFCs fuelled with hydrogen and carbon monoxide. All irreversible effects including mixing is generally described by an exergetic efficiency $\zeta < 1$. The detailed reasons for any irreversibility of the SOFC and other components are not important for the description of the system's behavior if they are only considered properly in the system. The only important ratio here is the ratio between work and heat within the single components and the temperatures of the heat sources and the heat sinks. The SOFC is the heat source of the fuel processing, i.e., reforming and evaporation delivers the internal heat sinks.

For the present analysis, the SOFC is the heat source of two or three Carnot cycles, and the reformer and the evaporator are their heat sinks in the reversible case. The real engines are: the heat engine HE1, operating between the SOFC and the reformer, and the heat engine HE2, operating between the SOFC and the evaporator. Finally, a third heat engine HE3 must operate between the SOFC and the ambient state if the waste heat of the SOFC is not used completely in the system. All real heat engines are described as Carnot-type engines with an exergetic efficiency <1. The flue gas flow is divided into two streams. The air is heated in the air heater AH by cooling the major stream of the flue gas (FGC). The reactant feed water (of reforming) is heated in the economizer from the ambient temperature T_0 to the evaporator temperature T_{evap} and the saturated steam is superheated from T_{evap} to the reformer temperature T_{ref}. The reactant methane is heated in the fuel heaters FH1 and FH2 from the ambient state T_0 to the reformer temperature T_{ref} and finally the products (of reforming) hydrogen and carbon monoxide (+steam) are heated from T_{ref} to T_{SOFC} in the product heater PH. The required heat is supplied by the cooling of the second pass of the flue gas (FGC) from T_{SOFC} to a waste gas temperature $>T_0$, by the SOFC directly (for PH), by the waste heat of HE1 (for $T < T_{\mathrm{ref}}$) and by the waste heat of HE2 (for $T < T_{\mathrm{evap}}$). An auxiliary burner must be used for the reforming process if the waste heat of the SOFC cannot cover the heat requirement of the reformer and the evaporator. This auxiliary burner is not shown in Fig. 8. The use of efficiencies $\eta < 1$ as the ratio of used and supplied heat allows a realistic description of HEX, burners and other thermal components within the entire system. The internal reforming in the SOFC is included in this modeling of the system ($T_{\mathrm{SOFC}} = T_{\mathrm{ref}}$). The external reforming is included in this model as well if the heat engine HE1 is replaced by a burner.

The parameters listed in Table 1 have been used for an analysis of the both systems as standard values, some have been varied ceteris paribus for different analysis.

The system efficiencies η_{syst} of combined SOFC cycles with integrated and external reforming have been calculated and compared by using the general model of Fig. 8 [5,6]. With the given assumptions for this analysis, typical results are shown in Fig. 9. The possible system efficiencies η_{syst} of systems with external reforming are about 7–8% lower than of a system with

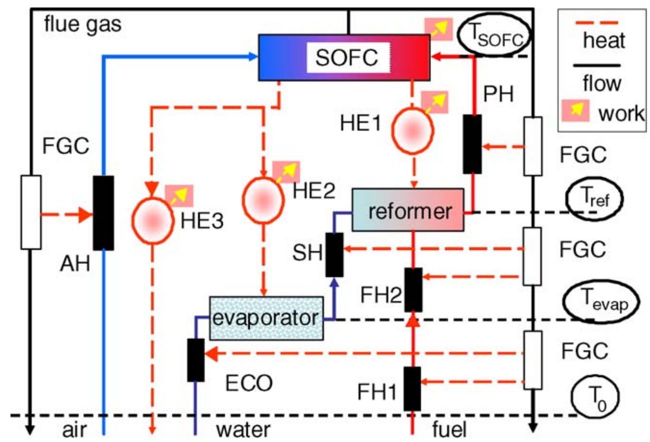

Fig. 8. Expanded reference cycle including fuel processing.

Table 1
Standard parameters for the analysis of SOFC hybrid cycles

SOFC temperature, T_{SOFC}	900 °C
Reformer temperature, T_{ref}	750 °C
Evaporator temperature, T_{evap}	200 °C
Ambient temperature, T_0	25 °C
Excess air, λ	2
Water surplus, n_W	2
Exergetic efficiency SOFC, ζ_{SOFC}	0.60
Exergetic efficiency heat engine, ζ_{HE}	0.70
Efficiency of air heater, η_{AH}	0.90
Efficiency of heat exchangers, η_{HEX}	0.98

integrated reforming. The differences between the processes with external or integrated reforming are caused by the different utilization of the waste heat of the SOFC within the system. Integrated reforming is characterized by the entropy recycling by using the waste heat of the SOFC for the reforming. External reforming systems use an external burner with an additional entropy production. This increases the usable heat of HE3 operating with the heat source SOFC and the heat sink environment and thus the waste heat of the system increases. Thus, the entropy cannot be recycled during external reforming. An internal reforming in the SOFC has no temperature difference available for a power generation during the heat transport. This leads to a slight decrease of the system efficiency η_{syst} of the internal reforming compared with the integrated reforming.

System efficiency and HEX area depend clearly on the excess air λ. The HEX efficiency η_{AH} of the air heater is an important parameter there. The system efficiency η_{syst} is thus plotted against the excess air λ in Fig. 10 with η_{AH} as a parameter. The system efficiency η_{syst} is independent of λ for $\eta_{AH} = 1$ as expected because a basic chemical thermodynamics approach shows that free reaction enthalpy $\Delta^r G$ is independent of the excess air λ. But η_{syst} decreases with increasing λ for all $\eta_{AH} < 1$. The influence of η_{AH} increases with increasing λ. The behavior of the system for $\eta_{AH} = 0.85$ is shown Fig. 10.

An increasing λ decreases the work of the heat engine HE3 by increasing heat losses and η_{syst} decreases slightly. η_{syst} decreases sharper from about an excess air $\lambda \approx 3$ because there is no heat for the operation of HE3. The waste heat of the SOFC can only supply the heat engines HE1 and HE2 operating between the

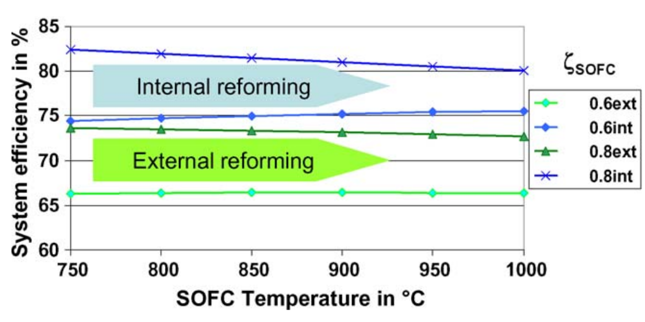

Fig. 9. Influence of the system integration of reforming on the system efficiency. $\zeta_{HE} = 0.7$; excess air $\lambda = 2$; excess water $n_W = 2$; $T_{ref} = 750$ °C; $T_{evap} = 200$ °C.

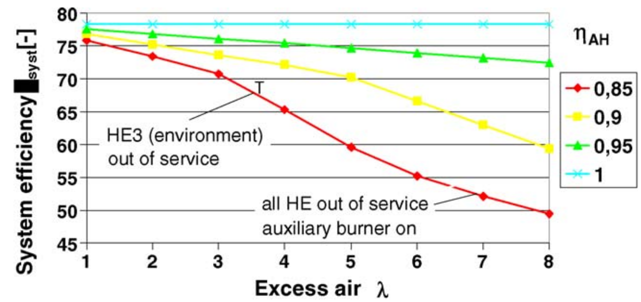

Fig. 10. The influence of the excess air λ and the HEX efficiency η_{AH} of the air heater on the system efficiency η_{syst} of SOFC–heat engine hybrid cycles. $\zeta_{SOFC} = 0.6$; $\zeta_{HE} = 0.7$; water surplus $n_W = 2$; integrated reforming $T_{SOFC} = 900$ °C; $T_{ref} = 750$ °C; $T_{evap} = 200$ °C.

SOFC and the reformer and the evaporator, respectively, caused by the increasing heat loss of the air heater. The decrease of the system efficiency η_{syst} with an increasing λ in the region $3 < \lambda < 6$ becomes sharper. Finally, in the region $\lambda > 6$ there is no heat engine in operation and all additional heat losses must be compensated by the auxiliary burner. η_{syst} drops to values lower than 50% as shown in Fig. 10.

Fig. 10 shows clearly the influence on the system efficiency of the excess air λ and the HEX efficiency η_{AH} of the air heater. But it gives no indication on the HEX area needed. Fig. 11 shows thus the influence of the excess air λ on the internally exchanged heat again with the HEX efficiency η_{AH} of the air heater as a parameter. The internally exchanged heat is related on the produced power of the system. This internally exchanged heat to power ratio increases with the increasing excess air and the decreasing HEX efficiency η_{AH} of the air heater. The influence of the decreasing system efficiency is thus stronger than the influence of the reduction of η_{AH}. A decreasing system efficiency increases the fuel flow and increases thus the related air flow, connected with an increase of the internally exchanged heat. This effect stops when the auxiliary burner is needed to supply the increasing heat losses. At this operation the SOFC is the only power generator and its cooling is determining the excess air λ. But the additional fuel consumption of the auxiliary burner is using the depleted air from the SOFC system and the excess air λ_{outlet} at the systems outlet is than lower than λ. This is the reason why the curve of

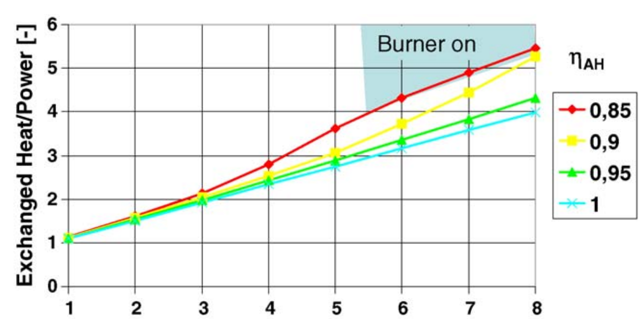

Fig. 11. Excess air, exchanged heat and HEX area.

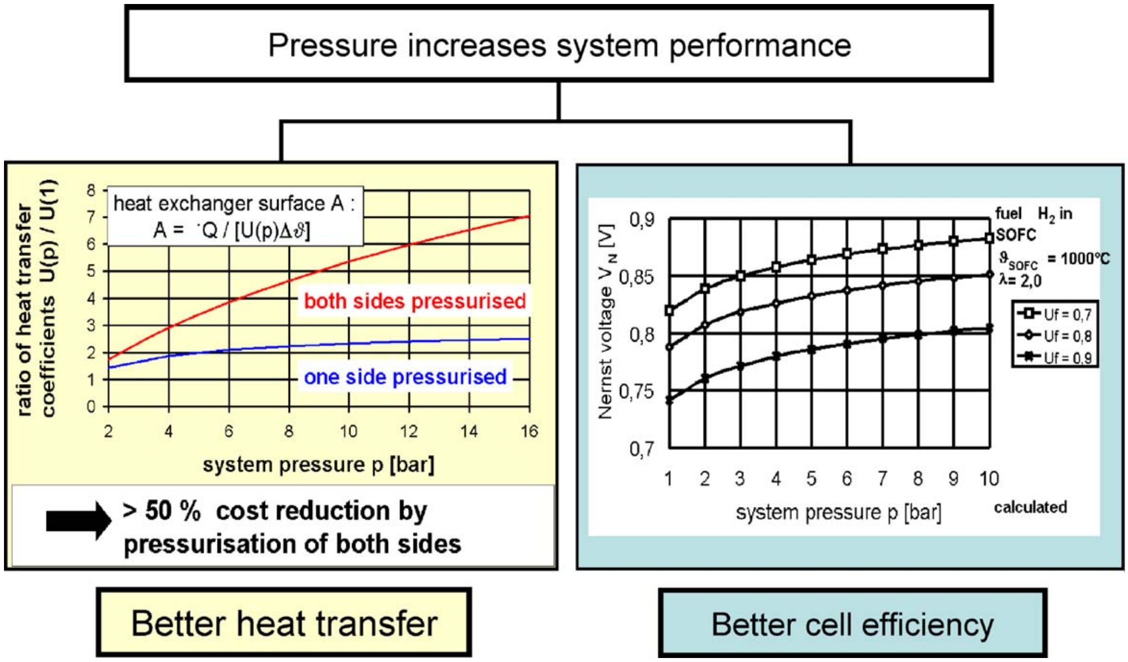

Fig. 12. The influence of pressurization on needed area.

the internal exchanged heat to power ratio changes its shape at $\eta_{AH} = 0.85$.

4.2. Influence of BoP components

The strategy of reducing the needed area to save weight and cost can be supported by an adequate design and operation of the components. The influence of pressurization is considered in Fig. 12.

The pressurization of a SOFC system has mainly two effects. It increases the heat transfer coefficient by about two if only one side of the HEX is pressurized and by up to seven or more if both sides are pressurized. The reference case is the ambient state on both sides of the HEX. This increase of the heat transfer coefficient is connected with a decreasing demand on HEX area. The direct influence on the HEX area is shown at the left side of Fig. 12. But the second effect of pressurization is the increase the cell efficiency represented by the Nernst voltage at the right side of Fig. 12. Again an increasing pressure is reducing the HEX area because the better cell efficiency reduces the demand on fuel and thus the air flow as already discussed above. Considering these effects we can conclude that the increase of pressure has generally the benefit of an increasing efficiency and a reduced demand on HEX area.

The pressurization also increases the power density at a certain cell voltage as shown in Fig. 13 [7]. The polarization losses are not really influenced by the pressure in a pressure range from 15 to 1 bar. The cell performance is thus mainly influenced by the reversible work of hydrogen oxidation in this range of pressure. At a pressure <1 bar the diffusion overpotential at the cathode could increase disproportionate.

The left part of Fig. 13 shows the influence of the pressure on the power density and the right part the connection of power density and stack cost. Again instead of cost there could be the weight per square meter of the cell as well. The power density increases with an increasing pressure at a constant cell voltage and the power related cost decrease significantly. If the power density is kept constant a higher voltage can be tapped at higher pressures. In this case, the power related cost do not change. On the one hand, the required cell area decreases and the efficiency increases with higher voltages for a fixed performance. But on the other hand, the cell degradation increases with lower voltages. The choice is thus depending on the application.

But an increase of the electrochemical losses during lifetime can decrease the power density of the cell. The cell power density of a fuel cell depends on the internal resistances, which are influenced by activation, concentration and ohmic caused polarizations as shown in Fig. 14. Its left side contains the influence of the internal resistance on power density and voltage and its left side again the influence on power related cost. The power density increases with a decreasing internal resistance at a constant

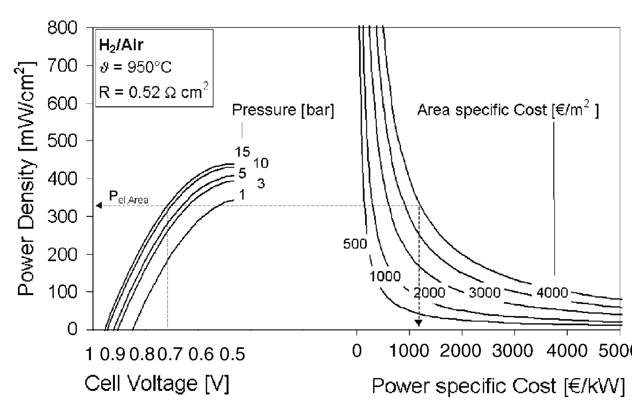

Fig. 13. Influence of pressurization on cell power density.

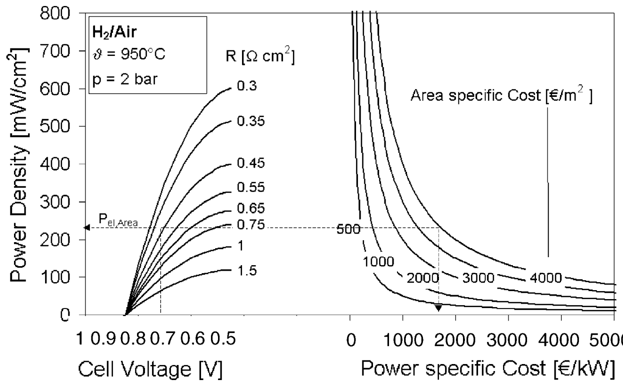

Fig. 14. Influence of the internal resistance on the cell power density.

cell voltage. Again the power related cost decrease at constant area related cost, independent of the improvement of the cell resistance. Otherwise a higher voltage can be reached at a lower resistance if the power density remains constant. In this case, the power specific cost is constant if the area specific cost does not change.

The influence of the isentropic compressor and turbine efficiency on system efficiency is investigated for a simple SOFC-GT cycle fed with methane. The simple SOFC-GT cycle consists of a SOFC stack with an integrated reformer and air pre-heater. The excess air is chosen as constant with 1.44 and the pressure ratio with 15 in this example. This cycle reaches an electrical efficiency of about 68% (LHV) at a system pressure of 15 bar, an average cell voltage of 0.7 V, a fuel utilization of 85% and turbine inlet temperature of 920 °C. This is a not optimized choice of thermodynamic parameters just to show relation between the isentropic efficiencies and the system efficiency. The isentropic efficiencies of the compressor and the turbine are varied from 55 to 95% as shown in Fig. 15. This variation gives an overview of the turbo machinery scaling effect and system scaling effect, respectively. A system efficiency of 65% needs already an isentropic efficiency of about 80%, small units might reach a lower system efficiency only.

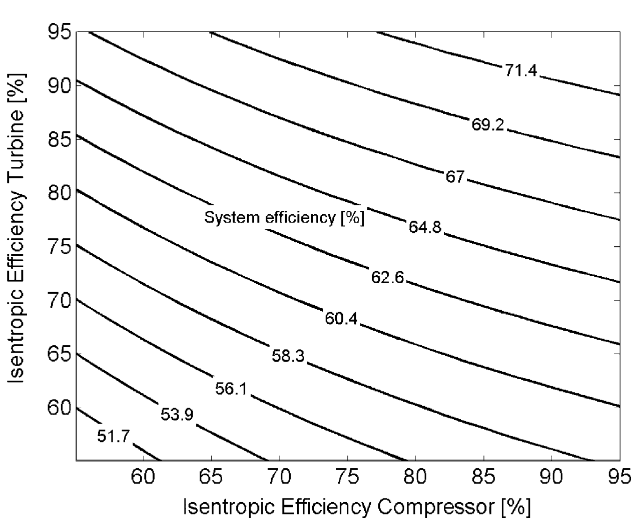

Fig. 15. Variation of isentropic efficiency of compressor and turbine.

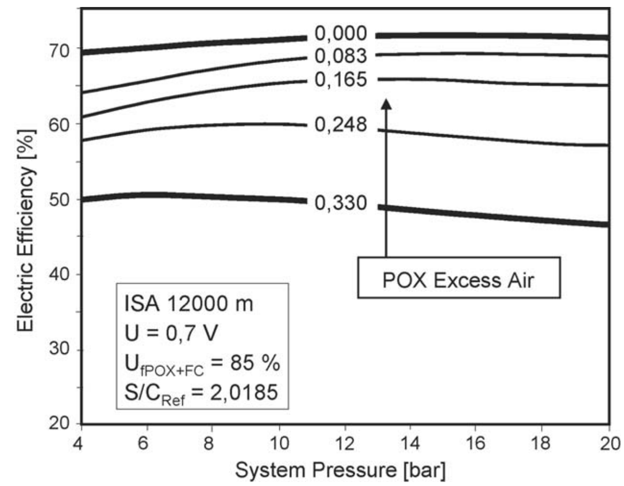

Fig. 16. Influence of excess air POX on system efficiency.

The use of higher hydrocarbons as fuels like kerosene or diesel the choice of fuel processing becomes a high influence on system efficiency. This is caused by the possible combination of an exothermal POX – producing an extra amount of entropy – with the endothermal reforming process. The influence of the excess air needed for the POX-based design on the electric efficiency is shown as a function of the system pressure in Fig. 16 [8]. The excess air of the POX is a measure for the entropy production. The influence of the system pressure (and thus the influence of altitude) is small compared with the influence of the excess air of the POX. Thus, these results are valid for maritime applications as well. Fuel processing by POX delivers the lowest efficiency of about 50% while a full integrated reforming delivers an efficiency of almost 70%. This result is not unexpected because the combustion process of the POX produces an extra amount of entropy and the excess air for cell cooling has to be increased with the consequence that the waste gas loss and the parasitic losses increase as well [9].

5. Experimental results and development projects

5.1. Worldwide status of industrial hybrid programs and projects

5.1.1. Solid-state energy conversion alliance (SECA)

The application of fuel cell systems and ultimately fuel cell + turbine (FCT) hybrids is limited largely by the high cost of the fuel cell. To address the cost issue, the US DOE is implementing the SECA program. The SECA program is dedicated to developing innovative, effective, low-cost ways to commercialize SOFCs. NETL is partnering with Pacific Northwest National Laboratory (PNNL) in developing new directions in advanced materials, processing and system integration research under the SECA initiative for the development and commercialization of modular, low-cost and fuel flexible 3–0-kWe SOFC systems by 2010 (Fig. 17).

DOE has estimated that a 5-kWe planar SOFC system can reach US$ 400 kW^{-1} at reasonable manufacturing rates. With this low-cost, the SOFC has the potential to move out of

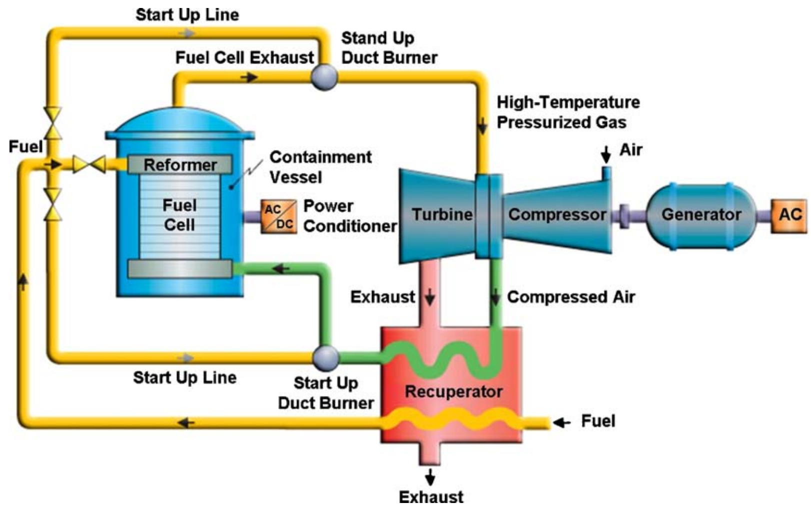

Fig. 17. Direct FCT hybrid.

limited niche markets into widespread market applications. If a common module can be produced for these widespread markets, one can achieve the high volume needed to reduce costs. This approach is called "mass customization." In addition, if the modular 3–10 kWe units can be scaled-up and aggregated to larger sizes with no increase in cost, then commercial, micro grid and other distributed generation markets, as well as central station, will be attainable. SECA developed technologies will provide the basis for the development of SECA-based SOFC FCT hybrid systems that achieve 60% electrical efficiency and near zero emissions when integrated in FutureGen power plants. Current SECA industrial team participants include General Electric, Siemens Westinghouse, FuelCell Energy, Delphi, Cummins Power Generation and Accumetrics.

5.1.2. Solid oxide fuel cell hybrid system for distributed power

The Hybrid Power Generation Systems Division of General Electric is collaborating with DOE/NETL to develop SOFC/gas turbine hybrid systems for distributed power generation applications. The objectives for this project are to analyze and evaluate SOFC/gas turbine system concepts. Technical barriers in pressurization and scale-up of preliminary design concepts will be resolved for both the feasibility demonstration system and the conceptual system. A preliminary design for high-temperature heat exchangers for hybrid system applications has been developed, and pressurized operation of SECA-type planar SOFC stacks has been demonstrated. The SOFC is based on thin-film electrolyte technology fabricated with the tape calendaring method and thin-foil metallic interconnects leading to a low-cost, high-performance, compact planar SOFC. The gas turbine is based on commercial products. The proposed hybrid system has a potential for efficiency greater than 65%.

5.1.3. 220-kWe pressurized hybrid demonstration

A 220-kWe FCT hybrid demonstration was recently completed through a multi-year collaborative effort led by Southern California Edison in partnership with Siemens-Westinghouse Power Corporation (SWPC), DOE/NETL and the University of California at Irvine's National Fuel Cell Research Center. The project was the world's first demonstration of a pressurized SOFC generator, and the world's first demonstration of a SOFC coupled with a microturbine generator (MTG). The SOFC stack was contained in a pressure vessel and operated at 3 atm (absolute) pressure and a temperature of 1000 °C. The hot, high-pressure exhaust gas from the SOFC generator drove an Ingersoll-Rand 70-kWe MTG. The SOFC stack produced 170-kW DC and the MTG produced 20-kW net AC. The system accumulated more than 3200 h of run-time, while operating at a calculated net AC electrical efficiency of 53%. Pre-commercialization efforts by SWPC are being redirected to smaller sizes for combined heat and power applications.

5.1.4. 300-kWe atmospheric hybrid demonstration

DOE/NETL and FuelCell Energy (FCE) are working collaboratively to develop and demonstrate an atmospheric molten carbonate Direct FuelCell/Turbine (DFC/T) hybrid system. To date, the R&D efforts have resulted in significant progress in validating the DFC/T cycle concept. FCE has completed successful proof-of-concept testing of a DFC/T power plant based on a 250-kWe DFC integrated initially with a Capstone 30-kWe and then a 60-kWe modified MTG (see Figs. 18 and 19). The subMW system tests have accumulated over 6800 h of successful operation with efficiency of 52%. This proof-of-concept demonstration has provided information for the continued design of a 40-MWe DFC/T power plant that is expected to approach 75% efficiency (LHV natural gas), as well as to serve as a platform for optimization of subMW class DFC/T hybrid systems. One of the significant challenges for this technology is the development of high temperature heat exchangers that offer differential pressure operation. Pre-commercial subMW alpha and beta units will be demonstrated over the next 2 years.

SOFCs will operate on today's conventional fuels such as natural gas, diesel, coal and gasoline, as well as hydrogen, the fuel of tomorrow. The SECA program will provide a bridge to the hydrogen economy beginning with the introduction of SOFCs

Fig. 18. FCE SubMW hybrid.

for stationary (both central generation and distributed energy) and auxiliary power applications. One of the most promising ways to produce hydrogen in the U.S. may be with coal. Coal is a very abundant resource in the U.S. and will be the primary fuel if energy independence is to be realized. Over 50% of the electricity in the U.S. comes from coal, and coal use is increasing. The President recently announced the FutureGen project to produce hydrogen from coal. This is a US$ 1 billion Presidential initiative leading to a 10-year demonstration project to create the world's first coal-based zero-emissions power plant. Around US$ 9 million in initial funding has been received in 2004.

From the perspective of fuel cells, the goal is to aggregate SECA fuel cells into larger systems and to produce a very high-efficiency FCT hybrid module as a key part of FutureGen. The highly efficient SOFC hybrid module will produce electric power while other integrated subsystems produce hydrogen and sequester CO_2. The hydrogen produced can be used in fuel cell cars and for large SOFC distributed generation applications. The fuel cell or hybrid could operate on syngas or hydrogen, and segregation or isolation of CO_2 can be achieved during syngas operation with some fuel cell designs (see Figs. 18 and 19) [10]. DOE is continuing the development of hybrid systems for coal plants and will be selected major hybrid developers to work to develop and demonstrate fuel cell hybrids through 2015.

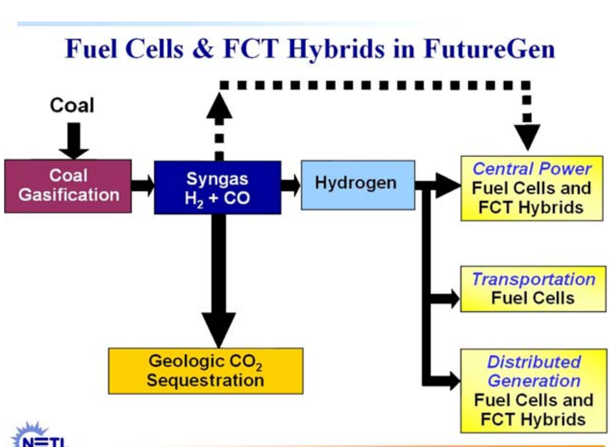

Fig. 19. Fuel cells and FCT hybrids in FutureGen.

DOE/NETL and the National Fuel Cell Research Center are developing and analyzing cycles capable of achieving 75% fuel-to-electrical efficiency on natural gas (LHV) and 60% on coal (HHV) for large (~300 MW) central power plants [11]. In both cases, cycles have been identified that are capable of achieving these efficiency goals for advanced power systems like FutureGen. FCT hybrid systems are key to these cycles.

5.2. NETL in-house experimental simulator and results

An experimental hardware in the loop hybrid fuel cell gas turbine simulation facility has been constructed by the Energy System Dynamics Division within the Office of Science, Technology and Analysis at NETL. The primary objectives of the Hybrid Performance (Hyper) project at NETL are to identify component technology issues and to investigate critical operability issues inherent in hybrid fuel cell systems. The Hyper facility at NETL is a hardware simulation of a fuel cell gas turbine hybrid power system capable of emulating systems in the range of 300–900 kW. The hardware portion is comprised of a modified single-shaft gas turbine, a high-performance exhaust gas recuperator, several pressure vessels that represent the volumes and flow impedances of the fuel cell and combustors, and the associated integration piping. The simulation portion consists of a real time fuel cell model that is used to control a natural gas burner, which replicates the thermal output of a solid oxide fuel cell. This approach allows for the development of validated models and control architectures that can avoid potential issues with load following and load shedding scenarios. The facility will ultimately accommodate a variety of fuel cell gas turbine configurations, but will initially focus on a direct-fired solid oxide fuel cell gas turbine configuration. A more detailed description of the facility has been presented previously [12]. The facility is open to researchers for collaboration and a simplified process flow diagram is illustrated in the Fig. 20 below.

Current experimental work has focused on the use of air control to manage the needs of the FCT system. Several control strategies have been investigated, including cathode air control, and compressor bleed-air control. Managing cathode air flow during a load transient imposed on a SOFC/GT hybrid is critical to the operability of the power system. Any sudden reduction in load on the fuel cell would require a corresponding reduction in cathode cooling flow to prevent over-cooling the fuel cell, which could lead to thermal fracture of the ceramic stack components. At the same time, the turbine in the system must deal with a sudden increase in thermal energy due to combustion of the increased amount of fuel passing unutilized through the fuel cell. This necessitates the use of a supplementary sink or source of energy to the hybrid plant in offsetting any transients. The implementation of by-pass valves to manage cathode air flow in parallel flow loops was tested and the limits of the hybrid system components operation were evaluated using the Hyper facility.

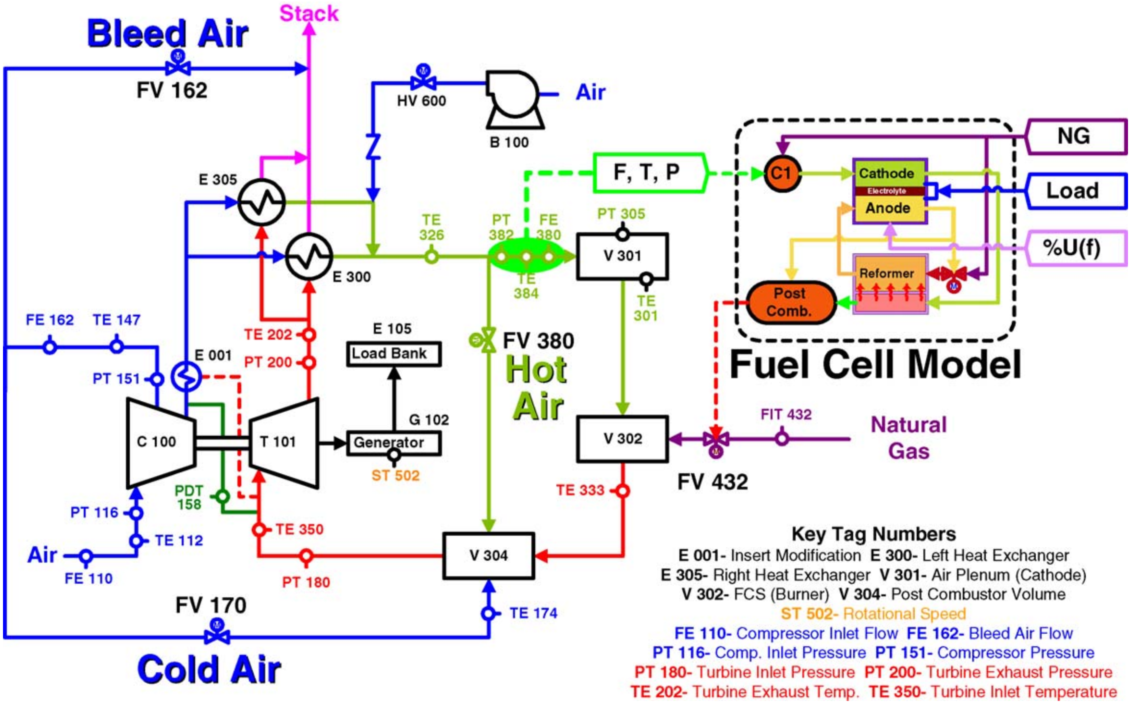

Fig. 20. The Hybrid Performance project facility simplified process flow diagram.

A detailed discussion of the experimental procedure has been previously presented [13].

The use of compressor bleed (FV-162 in Fig. 20) is compared to the use of cold air by-pass (FV-170 in Fig. 20) in Fig. 21 below. Both valves were operated to the extent of system limits with the turbine. In order to separate various coupled phenomena, the work assumed a fixed fuel cell operation in spite of any change in cathode flow, and employs a fixed gas turbine generator output of no electrical load. Compressor bleed air was limited to about 23% of the total inlet flow because the turbine exhaust gas temperature limit was reached at this point. The cold air by-pass valve could be opened to by-pass as much as 62% of the total inlet flow, and was limited only by the pressure drop across that flow loop.

The data are presented in terms of the fuel required to divert air flow from the cathode expressed as a percent of fuel required for the case without any by-passed flow. Compressor bleed air is shown to require a much greater specific energy requirement, while cold air by-pass is shown to have an insignificant specific energy requirement over the same operable range of by-passed flow.

The huge increase in energy requirement shown for the case of compressor bleed indicates that it would be an effective means of absorbing a thermal transient impacting the turbine in the system. The data for the cold air by-pass shows that it would be an effective means of controlling cathode air flow without a significant penalty in system efficiency. Both control strategies are complimentary and will play an important role in managing transient operation of fuel cell-turbine hybrid power systems.

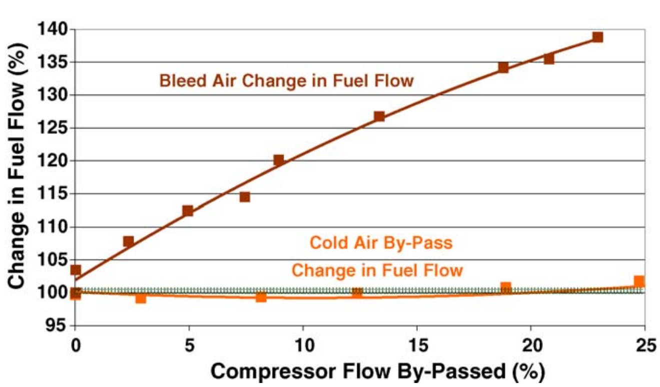

Fig. 21. A comparison of modeled compressor pressure vs. measured compressor pressure during a Hyper system startup.

5.3. GT development for SOFC-GT

Similar to a recuperated turbine cycle, the turbine in a hybrid cycle is characterized by relatively low operating pressure ratios and low operating temperatures. From this perspective, minimal effort should be required for development of a turbine for a hybrids application, and the U.S. DOE is not currently dedicating resources to address this issue. However, work conducted at NETL using the Hyper research facility has indicated that compressor dynamics are greatly impacted by the integration of substantial volume and pressure drop in the main flow path between the compressor and turbine [14]. Testing conducted by Siemens Westinghouse and the National Fuel Cell Research Center at the University of California Irvine identified combustor development for co-firing with the capability for handling a wide range of fuel modulation (5–110%) as an area of required technology development for turbines in hybrid cycles [15].

Previous cycle analysis work conducted at the Georgia Institute of Technology has shown that a reduction in fuel utilization of the fuel cell in a hybrid configuration has minimal impact on system efficiency, suggesting that a wider range of nominal turbine inlet temperature is possible in the turbine design [16]. Cycle analysis will have to be carefully considered in the course of turbine development for fuel cell gas turbine hybrids.

6. Conclusions

FCT hybrid power systems offer the highest efficiency and the cleanest emissions of all fossil fuelled power. The engineering for the highest possible efficiency at lowest cost and weight depends on general system architecture issues and the performance of the components. System studies, such as outlined in this paper, provide direction for the most efficient path toward achieving the most beneficial result for this technology. Ultimately, FCT systems applicable to integrated gasification combined cycle power systems will form the basis for reaching the goals for advanced coal-based power generation. The FCT hybrid power island will also be important for the FutureGen plant and will provide new options for carbon dioxide capture and sequestration as well as power and hydrogen generation.

Much work needs to be done to realize the potential shown for FCT systems. The US DOE is sponsoring several projects to begin understanding the unique requirements for these systems. One of these projects, Hyper, will provide information on FCT dynamics and will help identify technical needs and opportunities for cycle advancement. For example, this project has demonstrated the use of compressor bleed air and cold air by-pass for system control using valves only in side streams that do not see significant temperatures. The methods studied show promise for effective control of a hybrid system without the direct intervention of isolation valves or check valves in the main pressure loop of the system, which introduce substantial pressure losses, allowing for realization of the full potential efficiency of the hybrid system.

References

[1] W. Winkler, Analyse des Systemverhaltens von Kraftwerksprozessen mit Brennstoffzellen, Brennstoff-Wärme-Kraft 45 (Heft 6) (1993) S302–S307.

[2] W. Winkler, Der Einfluß der Prozeßkonfiguration auf das Arbeitsvermögen von Verbrennungskraftprozessen, Brennstoff-Wärme-Kraft 46 (Heft 7/8) (1994) S334–S340.

[3] W. Winkler, Preparing for future changes in power supply systems created by fuel cells—what measures can be taken to remain competitive? in: Proceedings of IIR Conference: Quantifying the Costs and Commercial Viability of Fuel Cell Technology for Power Generation, London, November, 1998.

[4] W. Winkler, Brennstoffzellenanlagen, Springer-Verlag, Berlin, 2002.

[5] W. Winkler, SOFC-integrated power plants for natural gas, Proceedings First European Solid Oxide Fuel Cell Forum, Ulf Bossel, Lucerne, October 3–7, 1994, pp. 821–848.

[6] W. Winkler, Lay out principles of the integration of fuel preparation in fuel cell systems, in: Proceedings of the Second IFCC (International Fuel Cell Conference), NEDO, Kobe, Japan, 1996, pp. 397–400.

[7] P. Nehter, Thermodynamische und ökonomische Analyse von Kraftwerksprozessen mit Hochtemperatur-Brennstoffzelle SOFC, Thesis TU Dresden, 2004.

[8] W. Winkler, P. Nehter, Aspects of process design of SOFC hybrid systems for aeronautic and maritime application., in: Proceedings of the Ninth International Symposium on Solid Oxide Fuel Cells, American Electrochemical Society, Que., Canada, 2005, pp. 229–239.

[9] W. Winkler, SOFC-integrated power plants for natural gas, in: Proceedings of the First European Solid Oxide Fuel Cell Forum, Ulf Bossel, Lucerne, October 3–7, 1994, pp. 821–848.

[10] U.S. Department of Energy, Office of Fossil Energy, FutureGen-Integrated Hydrogen, Electric Power Production and Carbon Sequestration Research Initiative, March, 2004.

[11] S. Samuelsen, Fuel Cell/Gas Turbine Hybrid Systems (www.asme.org/igti/resources/articles/turbo-fuel-cell_report_feb04.pdf).

[12] D. Tucker, E. Liese, J. Vanosdol, L. Lawson, R. Gemmen, Fuel cell hybrid simulator facility design, in: Paper Presented at the 2003 ASME IGTI Turbo-Expo, Atlanta, Georgia, June 15–19, 2003.

[13] D. Tucker, L.O. Lawson, R.S. Gemmen, Characterization of air flow management and control in a fuel cell turbine hybrid, in: Proceedings of the ASME Power Conference, PWR2005-50127, April, 2005.

[14] D. Tucker, L.O. Lawson, R.S. Gemmen, Evaluation of hybrid fuel cell turbine system startup with compressor bleed, in: ASME Turbo Expo, GT2005-68784, 2005.

[15] K. Litzinger, Critical hybrid component technologies—turbines, 4th Annual International Colloquium on Environmental Prefered Advance Power Generation/DOE, UN, EU Hybrid Fuel Cell Technologies, Irvine, California, September 21–22, 2005.

[16] C.L. Haynes, W.J. Wepfer, Enhancing fuel cell/gas turbine hybrid power systems via reduced fuel utilization within indirect internally reforming (IIR) fuel cell stacks, in: Proceedings of the ASME Advanced Energy Systems Division Publication AES, vol. 40, CD-ROM, ASME, New York, 2000.